

A Preliminary Study on Mapping the Regional Ionospheric TEC Using a Spherical Cap Harmonic Model in High Latitudes and the Arctic Region

Jingbin Liu¹, Ruizhi Chen¹, Heidi Kuusniemi¹, Zemin Wang², Hongping Zhang², Jian Yang³

¹ Department of Navigation and Positioning, Finnish Geodetic Institute, Geodeetinrinne 2, Masala, 02431, Finland

² Wuhan University, 129 Luoyu Road, Wuhan, 430079, China

³ School of Civil Engineering and Architecture, Wuhan University of Technology, 122 Luoshi Road, Wuhan, 430070, China

Abstract

The conventional ionosphere total electron content (TEC) models based on geodetic coordinates have asynchronous dimensional resolution, especially in the area close to the pole. This paper presents a novel spherical cap harmonic model for mapping the arctic regional ionospheric TEC in a spherical cap coordinate system. Utilizing a series of IGS (International GNSS Service) products, a set of dual-frequency GPS (Global Positioning System) data from IGS stations in high latitudes is processed and used to map the arctic regional TEC values with the spherical cap harmonic model and the conventional regional TEC models. Together with the global ionosphere mapping (GIM) model from IGS, the TEC mapping accuracies from these models are compared. The comparison results show that the spherical cap harmonic model has a better TEC mapping performance with more homogeneous accuracy distributions in both temporal and spatial domains for the arctic region. In addition, the spectrum components of the coefficient series of the spherical cap harmonic models are demonstrated in this paper.

Keywords: Spherical Cap Harmonic Model; Regional Ionospheric TEC model; Global Positioning System (GPS); High Latitudes and the Arctic Region; International GNSS Service (IGS)

1. Introduction

Human activities in high latitudes and the arctic region are nowadays more and more popular, e.g. resource utilization, research, airlines over the arctic, and exploration in the arctic region, etc. Therefore, accurate GNSS positioning and navigation in high latitudes and the arctic region is required for these applications. In this study, the high latitudes and the arctic region refer to the

region where the latitudes are higher than north 60 degrees.

The ionospheric effect is one major error source of GNSS positioning. The Klobuchar ionospheric model is broadcasted in the navigation data of the GPS signals, and used extensively to correct the ionosphere delay error. However, the Klobuchar model has just an overall accuracy of 50%~60% (Klobuchar 1996), and the remaining error may reach maximally dozens of meters in the line of sight direction.

Unlike the Equatorial region where the ionosphere is affected more directly by the solar activity, the ionospheric effect of the Arctic region is principally driven by the electron precipitation and the irregularities of electron density. Therefore, the ionosphere activity of the arctic region differs significantly with that of the equatorial region, e.g. the electron precipitation leads to the auroral light at night. As a consequence, in high latitudes and the arctic region, the ionosphere has much more irregularity than that of other regions, and the total electron content (TEC) of the ionosphere is even more difficult to be modelled due to two facts: on the one hand, the ionosphere TEC variation in the arctic region is much more complicated; and on the other hand, the conventional ionosphere models based on geodetic coordinates have asynchronous dimensional resolution, especially in the area close to the pole.

This paper proposes a spherical cap coordinate system based regional ionosphere model, referred to as the spherical cap harmonic model, to map the ionosphere TEC in high latitudes and the arctic region. This is the first study on mapping the TEC of the high latitudes and the arctic region with the spherical cap harmonic model, and a limited set of data is used considering the effect of first fact above. In order to avoid the impact of sharp solar activities on the ionosphere, this study just uses the

data of the first 90 days (from January to March) in 2007 when the Sun is in a calm period of its activity cycle and when the arctic region is in the period of polar nights.

Utilizing a series of IGS products, including e.g. the precise orbits of the satellites, differential code biases of satellites and receivers, and global ionosphere mapping (GIM), a set of dual-frequency GPS data from IGS stations in high latitudes and the arctic region is processed and used to map the regional TEC values with the spherical cap harmonic model and the conventional regional ionosphere models. For the purpose of comparison, GIM data is interpolated in spatial and temporal domains to generate the TEC at a given time and location.

In this paper, the mapping results of the spherical cap harmonic model are compared with that of the three conventional regional TEC models and the GIM interpolated model. The temporal and spatial distributions of the mapping accuracies of various models are analysed. The test results show that the spherical cap harmonic model has comparable overall accuracy with the conventional models in the region, and the spherical cap harmonic model performs better in the spatial domain as its accuracy is much more uniform over the entire region. And as the special feature of the spherical cap harmonic model, the zero-degree coefficient of the model indicates the TEC average of the region. Furthermore, in order to study preliminarily the periodicity of the ionosphere TEC in high latitudes and the arctic region, the discrete Fast Fourier Transformation (FFT) is computed for the time series of the coefficients of the spherical cap harmonic model, and the spectrum components are illustrated in this paper.

2. Mapping the Regional TEC with the Spherical Cap Harmonic Model

Most of the current TEC models are based on geographic coordinates (latitude and longitude) without considering the noncoherence of spatial scale. It is difficult to map the TEC at high latitudes and the arctic region with such models. Spherical cap harmonic model is an efficient approach to model the data over these regions using the spherical cap coordinate system.

2.1 Single layer model and mapping function

The single layer model is typically adopted for mapping the ionospheric TEC (Schaer 1999). It is assumed that all free electrons are contained in a shell of infinitesimal thickness. The altitude H of this idealized layer is usually set to 350 ~ 450 km, approximately corresponding to the altitude of maximum electron density. The ionosphere zone and the single layer model are illustrated in Fig. 1.

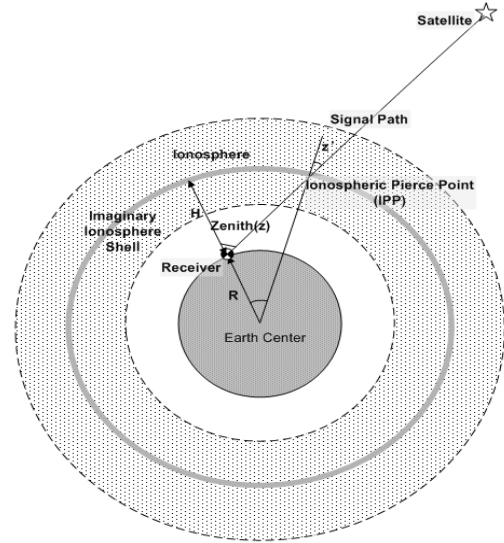


Figure 1: The Earth's ionosphere and the single layer model

The pierce point is the intersection of the single layer shell and the path of the GPS signal, z' is zenith distance of the satellite at the pierce point, and z is the zenith distance of the satellite at the location of the receiver. The geometric relationship between z' and z is given by:

$$z' = \arcsin \left[\frac{R}{R+H} \sin z \right] \quad (1)$$

where $R \approx 6371$ km is the mean radius of the Earth.

The following mapping function describes the ratio between the slant TEC (STEC) along the path of the GPS signal and the vertical TEC (VTEC) at the Ionosphere Pierce Point (IPP):

$$mf(z') = \frac{STEC(z')}{VTEC} \quad \text{with} \quad VTEC = STEC(0) \quad (2)$$

The mapping function $mf(z')$ is used to convert the STEC to the VTEC, or vice versa.

In this study, the height of the assumed single layer is selected as $H = 428.8$ km, which is close to the optimal approximation of the Chapman profile mapping function that has less than 1% of error (Schaer 1999), and the mapping function is a triangular function (Sardon et al. 1994) as:

$$mf(z') = 1 / \cos(z') \quad (3)$$

2.2 Carrier phase smoothing and variance estimation

The TEC values are the input or observations for estimating the coefficients of the spherical cap harmonic functions. In order to improve the accuracy of the TEC values derived from dual frequency pseudorange measurements, carrier phase smoothing is applied in this study.

At a given epoch k , the TEC value can be calculated by using either pseudorange or carrier phase measurements as follows (Liu 2008):

$$TEC_{p,k} = -\nu \times (P_2 - P_1) - \nu \times (B_{p,r} + B_p^s) \quad (4)$$

$$\begin{aligned} TEC_{\phi,k} &= \nu \times [\lambda_2(\phi_2 + N_2) - \lambda_1(\phi_1 + N_1) + B_{\phi,r} + B_\phi^s] \\ &= \nu \times (\lambda_2\phi_2 - \lambda_1\phi_1) + \nu \times (\lambda_2N_2 - \lambda_1N_1 + B_{\phi,r} + B_\phi^s) \end{aligned} \quad (5)$$

where $\nu = -f_1^2 f_2^2 / 40.28(f_1^2 - f_2^2)$, $f_i, \lambda_i (i=1,2)$ are the frequencies and wavelengths of two GPS carriers; $P_i, \phi_i (i=1,2)$ are pseudorange and carrier phase of dual frequencies; $N_i (i=1,2)$ are the ambiguities of carrier phase measurements; $B_{p,r}, B_p^s$ are the receiver and satellite inter-frequency hardware delay biases on the code measurements; $B_{\phi,r}, B_\phi^s$ are the receiver and satellite inter-frequency hardware delay biases on the carrier phase measurements. $TEC_{p,k}$ and $TEC_{\phi,k}$ are the TEC observations derived from pseudorange and carrier phase measurements at epoch k .

By re-arranging Eq. (4) and (5), a single parameter ΔTEC consisting of the unknown hardware delay biases and carrier phase ambiguities can be formed and estimated with pseudorange and carrier phase measurements as following:

$$\begin{aligned} \Delta TEC_k &= -\nu \times (B_{p,r} + B_p^s + \lambda_2 N_2 - \lambda_1 N_1 + B_{\phi,r} + B_\phi^s) \\ &= -\nu \times (P_2 - P_1 + \lambda_2 \phi_2 - \lambda_1 \phi_1) \end{aligned} \quad (6)$$

In the equations above, the ambiguities N_i are constant if cycle slips are not present or can be recovered. And as the inter-frequency hardware delay biases B are stable during a period of a few days (Schäfer 1999), the parameter ΔTEC hence is stable for a period of about one day. Therefore, the accuracy of this parameter can be improved using a recursive smoothing process over time as follows:

$$\Delta \tilde{TEC}_k = \frac{1}{K} \sum_{k=1}^K \Delta TEC_k = \frac{1}{K} \left(\sum_{k=1}^{K-1} \Delta TEC_k + \Delta TEC_K \right) \quad (7)$$

where k is the epoch number, and K is the total number of epochs ($k = 1, \dots, K$).

The smoothed ionospheric TEC can then be calculated with:

$$\begin{aligned} \tilde{TEC}_k &= \nu \times (\lambda_2 \phi_2 - \lambda_1 \phi_1) + \Delta \tilde{TEC}_k + \nu \times (B_{p,r} + B_p^s) \\ &= \nu \times (\lambda_2 \phi_2 - \lambda_1 \phi_1) - \frac{1}{K} \sum_{k=1}^K (\nu \times (P_2 - P_1 + \lambda_2 \phi_2 - \lambda_1 \phi_1)) + \nu \times (B_{p,r} + B_p^s) \\ &= \frac{K-1}{K} \times \nu \times (\lambda_2 \phi_2 - \lambda_1 \phi_1) - \frac{1}{K} \sum_{k=1}^K (\nu \times (P_2 - P_1)) \\ &\quad - \frac{1}{K} \sum_{k=1}^{K-1} (\nu \times (\lambda_2 \phi_2 - \lambda_1 \phi_1)) + \nu \times (B_{p,r} + B_p^s) \end{aligned} \quad (8)$$

Usually, the inter-frequency hardware delay biases are estimated as unknown parameters together with model coefficients. In order to apply the same set of hardware delay biases to different ionospheric models for comparison reason, the biases are estimated independently in this study. The smoothed TEC measurements are corrected with the hardware delay biases before applying to estimate the spherical cap harmonic model. According to Eq. (8), the smoothing process has no impact on the hardware delay biases, which are taken as constant.

Based on the assumption that pseudorange and carrier phase measurements are uncorrelated, the root mean square error (RMS) of the smoothed TEC observations can be estimated with the error propagation law as:

$$\begin{aligned} \sigma_{\tilde{TEC}_k} &= \sqrt{\left(\frac{K-1}{K} \right)^2 \sigma_{TEC_\phi}^2 + \frac{1}{K^2} \sum_{k=1}^K \sigma_{TEC_p}^2 + \frac{1}{K^2} \sum_{k=1}^{K-1} \sigma_{TEC_\phi}^2 + \sigma_B^2} \\ &= \sqrt{\frac{K-1}{K} \sigma_{TEC_\phi}^2 + \frac{1}{K} \sigma_{TEC_p}^2 + \sigma_B^2} \end{aligned} \quad (9)$$

where $\sigma_{TEC_p}^2, \sigma_{TEC_\phi}^2$ are the variance of TEC measurements derived from pseudorange and carrier phase, respectively, and σ_B^2 is the variance of hardware delay biases. This RMS estimated with Eq. (9) is used to calculate the weight of the TEC measurements in the least squares solution. Taking the accuracies of 0.3 m for the P-code pseudorange measurements and 0.05 cycles for the carrier phase measurements into account, the RMS of the pseudorange derived TEC measurements is $\sigma_{TEC_p} = 3TECU$, while that of the carrier phase derived TEC measurements is $\sigma_{TEC_\phi} = 0.1TECU$. To avoid the overweighting of smoothed TEC measurements, a limit of $K \leq 112$ is applied to the smoothing process.

2.3 Coordinate system

Usually the ionosphere pierce point is in the geographic or geomagnetic coordinate system. Therefore, it has to be transformed into the spherical cap coordinate system. The spherical cap coordinate system is an earth-centered coordinate system (Haines G.V. 1985). The pole of the spherical cap is chosen to define the coordinate system. The meridian passing through the spherical cap pole and the Antarctic pole is defined as the meridian of zero longitude in the spherical cap coordinate system. Fig. 2 illustrates the relationship between the geographic coordinate system and the spherical cap coordinate system.

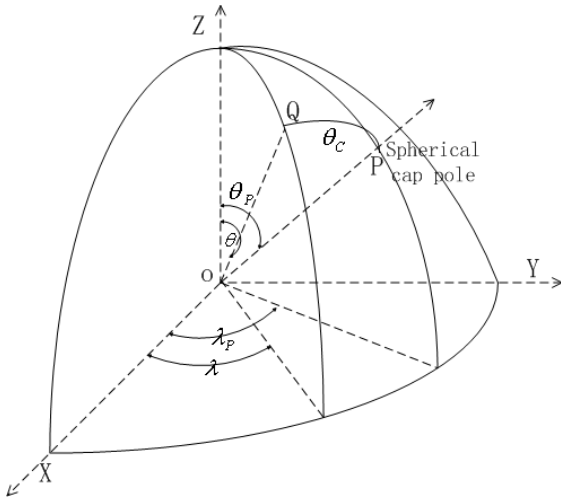


Figure 2: Coordinate transformation between geographic coordinate system and spherical cap coordinate system

As shown in Fig. 2, if the geographic colatitude and longitude of the pole P of the spherical cap are (θ_p, γ_p) respectively, the geographic latitude and longitude (β, γ) of any point Q can then be transformed into spherical cap latitude and longitude (β_c, γ_c) using:

$$\begin{cases} \beta_c = \arccos[\cos\theta_p \cos\theta + \sin\theta_p \sin\theta \cos(\gamma_p - \gamma)] \\ \gamma_c = \arcsin\left[\frac{\sin(\gamma - \gamma_p) \sin\theta}{\sin\theta_c}\right] \end{cases} \quad (10)$$

where the colatitudes $\theta = 90^\circ - \beta$ and $\theta_c = 90^\circ - \beta_c$.

For high latitudes and the arctic region, the pole of the spherical cap is set to the arctic pole, i.e. $(\theta_p, \gamma_p) = (90^\circ, 0^\circ)$, so the coordinate transformation is simplified.

2.4 The spherical cap harmonic model

A spherical cap is a part of the sphere with a co-latitude range from zero to θ_0 , as shown in Fig. 3.

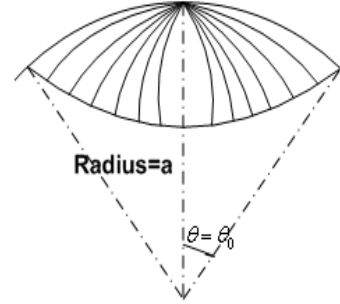


Figure 3: A spherical cap with a radius (a) and a half angle θ_0

The spherical cap harmonic model for mapping the regional TEC is expressed as:

$$E_v(\theta_c, \gamma_c) = \sum_{k=0}^{K_{MAX}} \sum_{m=0}^{\min(k, M)} \tilde{P}_{n_k(m)}^m(\cos\theta_c) [\tilde{C}_k^m \cos(m\gamma_c) + \tilde{S}_k^m \sin(m\gamma_c)] \quad (11)$$

where (θ_c, γ_c) is the spherical cap colatitude and longitude of the ionosphere pierce point, $E_v(\theta_c, \gamma_c)$ is the vertical TEC at the IPP (θ_c, γ_c) , K_{MAX}, M are the maximum degree and order of the series, $n_k(m)$ is the non-integer degrees, $\tilde{P}(\cos\theta_c)$ is the normalized associated Legendre function, $\min(k, M)$ is the minimal between k and M , and $\tilde{C}_k^m, \tilde{S}_k^m$ are the normalized coefficients of spherical cap harmonic model.

In the case of spherical cap ($\theta_0 \neq \pi$), the boundary conditions of Laplace's equations are met by real degrees $n_k(m)$ rather than integer degrees in the case of the globe. The real degrees $n_k(m)$ are solved by an iterative bisection solution, and k are the index of the real degrees ($0 \leq k \leq K_{MAX}$). More mathematical representations on the spherical cap harmonic function and the real degrees solution can be found in Haines (1985, 1988) and Liu (2008).

In this study, the spherical cap pole is at the North Pole, and the half angle of the spherical cap is 30 degree. Taking the trade-off between the spatial resolution requirement and the computational load into consideration, the maximum degree (K_{MAX}) is determined as 8. Table 1 lists the non-integer degrees $n_k(m)$ for the case when the half angle $\theta_0 = 30^\circ$.

Table 1: Non-integer degrees $n_k(m)$ given the half angle $\theta_0 = 30^\circ$

$n_k(m)$ when $\theta_0 = 30^\circ$									
$k \backslash m$	0	1	2	3	4	5	6	7	8
0	0.011719								
1	4.078125	3.121875							
2	6.837891	6.836719	5.49375						
3	10.03125	9.713672	9.384375	7.754297					
4	12.90820	12.90703	12.37266	11.80313	9.962109				
5	16.00781	15.82207	15.61875	14.91738	14.1750	12.13477			
6	18.9375	18.93047	18.58359	18.225	17.3918	16.51172	14.28398		
7	22.03125	21.87041	21.7125	21.24551	20.76094	19.81348	18.80156	16.42148	
8	24.95215	24.95391	24.68613	24.4125	23.84004	23.23828	22.19414	21.05625	18.54727

2.5 The connection between sessions for smoothing

In order to enhance the TEC mapping accuracy, each spherical cap harmonic model will be adopted for a short time interval. Each day is divided evenly into 12 sessions with a session length of 2 hours. Taking the hour angles of the Sun into account, the TEC measurements in each session are represented by one model. Therefore, there are 12 sets of models for each day. To avoid large gaps between the models of two consecutive sessions, the TEC is taken as a function of latitude, longitude and time denoted as $f(\beta, \gamma, t)$, and the following constraint conditions are imposed on the spatial and temporal domains of the TEC function:

$$\begin{cases} f_i(\beta_g, \gamma_g, t_s) = f_{i+1}(\beta_g, \gamma_g, t_s), & i=1,2,\dots,11 \\ \partial f_i(\beta_g, \gamma_g, t_s) / \partial \beta = \partial f_{i+1}(\beta_g, \gamma_g, t_s) / \partial \beta \\ \partial f_i(\beta_g, \gamma_g, t_s) / \partial \gamma = \partial f_{i+1}(\beta_g, \gamma_g, t_s) / \partial \gamma \\ \partial^2 f_i(\beta_g, \gamma_g, t_s) / (\partial \beta \cdot \partial \gamma) = \partial^2 f_{i+1}(\beta_g, \gamma_g, t_s) / (\partial \beta \cdot \partial \gamma) \end{cases} \quad (12)$$

where $i=1,2,\dots,11$ is the session number, (β_g, γ_g) are the latitude and longitude of the constraint grids and t_s is the constraint epochs.

The third line of Eq. (12) actually contains the constraint condition on the temporal domain as the time difference is equivalent to the longitude difference (the difference of hour angles of the Sun). It should be noted that the constraint will degrade the mapping accuracy to some extent. Therefore, with these constraint conditions, the connection of consecutive sessions is relatively continuous and the degree of smoothing is depending on the constraint weight.

Fig. 4 demonstrates the smoothness of calculated TEC with estimated spherical cap harmonic models in one day. Slight gaps occur at the epochs when the sessions turn around, which are a trade-off of the mapping accuracy.

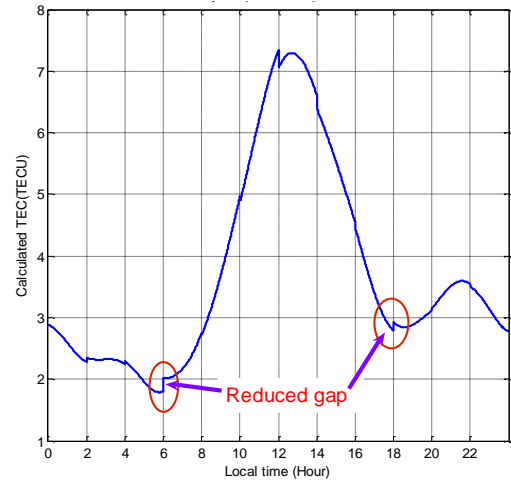


Figure 4: The daily profile of the calculated TEC with the constraint conditions between sessions

2.6 Conventional models for regional ionosphere TEC

In order to evaluate the performance of the spherical cap harmonic model, comparing with other regional ionosphere TEC models are conducted, including polynomial model, triangular series model, lower degree spherical function model and GIM interpolated model. This section describes the parameterization of these models in brief.

▪ **Polynomial model (POLY):** The polynomial ionosphere model has the expression (Liu et al. 2008a):

$$VTEC = \sum_{i=0}^n \sum_{k=0}^m E_{ik} (\beta - \beta_0)^i (S - S_0)^k \quad (13)$$

where (β_0, γ_0) is the geographical latitude and longitude of the central point of the region, S_0 is the hour angles of the Sun on the middle epoch of the observation session observed at the central point, S is the hour angles of the Sun of observation epochs at the IPPs, i.e.

$S - S_0 = (\gamma - \gamma_0) + (t - t_0)$, (β, γ) is the latitudes and longitudes of the IPPs, t is the observation epoch, t_0 is the middle time of the observation session, and E_{ik} are the coefficients to be estimated. In this study, the central point is chosen at $(\beta_0 = 75^\circ, \gamma_0 = 0^\circ)$, the degrees are $n = 4, m = 5$, and then the number of estimated parameters is $(n+1)*(m+1) = 30$.

▪ **Triangular series model (TRI):** The triangular series model is expressed as follows, which takes the TEC as the summation of the effects of different factors on the ionosphere (Georgiadous 1994):

$$VTEC = A_1 + \sum_{i=1}^{N_2} \{A_{i+1}\beta_m^i\} + \sum_{i=1}^{N_3} \{A_{i+N_2+1}h^i\} + \sum_{i=1, j=1}^{N_I, N_J} \{A_{i+N_2+N_3+1}\beta_m^i h^j\} + \sum_{i=1}^{N_4} \{A_{2i+N_2+N_3+N_I} \cos(ih) + A_{2i+N_2+N_3+N_I+1} \sin(ih)\} \quad (14)$$

where $h = \frac{2\pi(t_{sip} - 14)}{24}$

where A_i ($i = 1, 2, \dots, N_2 + N_3 + N_I * N_J + 2N_4 + 1$) are the parameters to be estimated, t_{sip} is the local time of the IPPs, h is a function of local time, β_m is the latitude of the IPPs. In this study, $N_2 = 0$, $N_3 = N_I = N_J = 1, N_4 = 6$, and the number of estimated model parameters is 15.

▪ **Lower degree spherical function model (LSF):** This model has the expression form of the spherical functions as follows (Wilson et al. 1995):

$$VTEC = \sum_{m=0}^M \sum_{k=0}^m (A_m^k \cos k * \gamma' + B_m^k \sin k * \gamma') P_m^k(\cos \beta) \quad (15)$$

where $\gamma' = \gamma_{IPP} + 15.0 * (UT - 12)$

where M is the degree of the spherical function, (γ_{IPP}, β) is the longitude and latitude of the IPPs, UT is the universal time at the IPPs, $P_m^k(\cos \beta)$ is the Legendre polynomials, and A_m^k, B_m^k are the model parameters to be estimated. In this study, the degree is chosen as $M = 4$, so there are 25 parameters to be estimated.

It should be pointed out that the lower degree spherical function model mapping the regional TEC is essentially different with the spherical harmonic model mapping the global TEC. Although they both have similar expression

forms, the spherical functions are not the solution of the Laplace's equation over the regional area any more, and are not the "harmonic functions".

▪ **GIM interpolated model:** As a benchmark, the GIM model is interpolated to generate the TEC in high latitudes and the arctic region. GIM is a global model published by IGS data analysis centers in IONEX format. The interpolation is operated at both spatial and temporal domains to obtain the TEC value at the given location and time. The methodology of spatial and temporal interpolation is described in Schaer et al. (1998).

These conventional models described in this section have not been developed for the arctic purposes, and they may be not practical in the arctic region. Next section will demonstrate the issues of these models when they are forced into the arctic region.

3. Mapping the Regional TEC in High Latitudes and the Arctic Region

The spherical cap harmonic model is applied to a GPS data set of three months (from January to March) in 2007 in this first study on ionospheric TEC of high latitude and the arctic region. In the period, the solar activity is relatively calm according to the Ap index in Fig. 5. Due to that polar nights occur in this period, the effect of solar activity on the ionosphere is minimized.

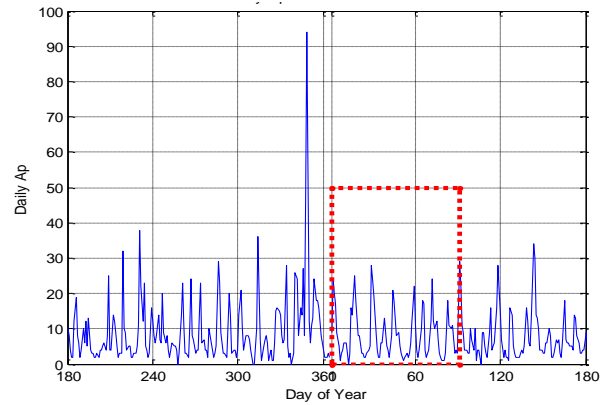


Figure 5: Daily Ap index from 180th day of 2006 to 180th day of 2007

The GPS data are observed at more than 40 IGS stations located at the region where the latitudes are higher than north 60 degree; the geographic distribution of these stations is illustrated in Fig. 6. The sampling rate of the GPS measurements is 30 seconds, and the cut-off elevation mask of 20 degrees is applied in the data processing.

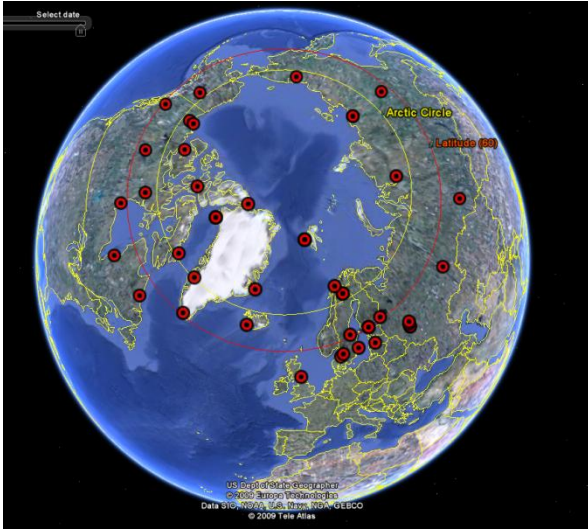


Figure 6: The geographic distribution of the IGS stations used in high latitudes and the arctic region based on Google Earth™

Through the data pre-processing process, some of the stations are removed from the list due to overall bad data quality or erroneous data formats, and some of the measurements are marked as outliers. The iterative smoothing process described in section 2.2 is performed to reduce the noise level of the TEC observations. And the weights of the TEC measurements in the least squares are evaluated according to the smoothed variances and the marks of outliers. For the reason of comparing the spherical cap harmonic model with other ionospheric models above, the same data set and pre-processing options are used for generating different models.

3.1 Overall residuals of the spherical cap harmonic model

Fig. 7 shows the daily residual and standard deviation (STD) of the spherical cap harmonic model, three conventional regional TEC models, and the GIM interpolated model in the observation period. The residual is defined as the difference between the model estimate and the smoothed TEC measurement from GPS observations above. In Fig. 7, five sub-figures are showing separately the residuals of the polynomial model (POLY), the triangular series model (TRI), the lower degree spherical function model (LSF), the spherical cap harmonic model (SCHA), and the GIM interpolated model in the order from the top to the bottom. In each sub-figure, the daily residual average is referred to as the left axes (“Residual Average”) and the daily residual standard deviation is referred to as the right axes (“Residual STD”). Table 2 lists the overall residual statistics for the entire observation period of 90 days.

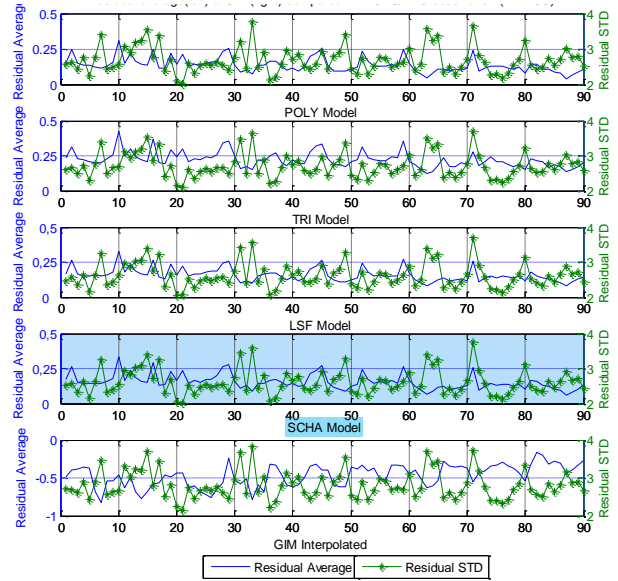


Figure 7: Daily TEC residual profile of the spherical cap harmonic model, the polynomial model, the triangular series model, the lower degree spherical function model, and the GIM interpolated model (in TECU)

Table 2: Residuals statistics of different mapping models for the entire observation period (in TECU)

Residual Statistics (in TECU)	Polynomial model	Triangular series model	Lower degree spherical function model	Spherical cap harmonic model	GIM interpolated model
Residual Mean	0.14	0.22	0.16	0.15	-0.47
Residual standard deviation	2.69	2.72	2.62	2.62	2.82

It should be pointed out firstly that the results of the polynomial model in Fig. 7 and Table 2 exclude the cases of mapping failures due to the boundary effect (see next section). According to Fig. 7 and Table 2, the spherical cap harmonic model, the polynomial model and the lower degree spherical function model have comparable accuracies in general, and the mapping results of these three models have no significant systematic biases.

3.2 Spatial distribution of the residuals

The spatial distribution of the mapping residuals is an indication of modelling quality over one large region. The residual at each grid point in this section is defined as the difference between the TEC value estimated with a regional model and that interpolated with the GIM model, different with section 3.1.

The polynomial model expression takes the region as one plane; however, the region of high latitudes has obvious distortion of one plane. This causes large mapping errors in the boundary area of the region. Fig. 8

demonstrates typically the instance of mapping failure using the estimated model of a session over a $5^\circ \times 5^\circ$ grid of high latitudes and the arctic region. In Fig. 8, the TEC values at the grids are calculated using a set of the coefficients of the polynomial model, and a red dot indicates the mapping failure case at the accompanying grid. The mapping failure means that the calculated TEC with an estimated model is negative or has a difference of more than 200 TECU with the estimated TEC of the GIM model at someone point. The mapping failure occurs in the area far away from the central point, and there are more cases at higher latitudes. Actually, when the latitude is 90 degrees, the points with different longitudes converge into the same point. However, the conventional regional models do not take this fact into consideration and have different results for the same point due to the spatial inhomogeneous resolution.

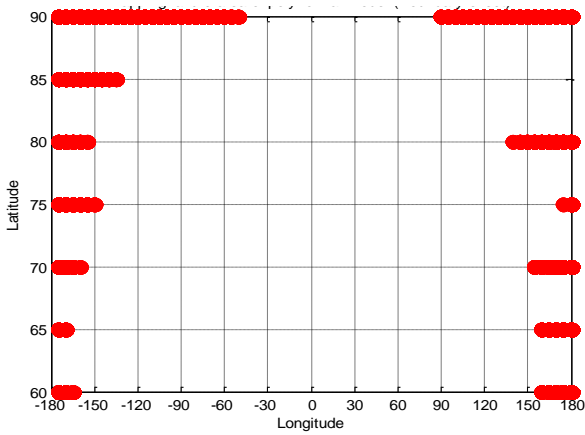


Figure 8: Mapping failure grid points (in red) of the polynomial model, referred to as the “boundary effect”

Fig. 9 shows the spatial distribution of the residuals of the spherical cap harmonic model over a $5^\circ \times 5^\circ$ grid. It is assumed that the spatial distribution of the mapping errors of the GIM model is more homogenous in high latitudes and the arctic region as it is a global model. Although the GIM model contains residual errors and an insignificant systematic bias (-0.47 TECU) as listed in Table 2, the spatial distribution of the model residuals derived with this approach is still a good indication of the mapping quality of a regional model.

As explained in Liu (2008), the residuals of the polynomial model at the boundary areas are more significant than at the grid points around the central point. This is referred to as the “boundary effect” from this point forward. As shown in Fig. 9, the boundary effect of the spherical cap harmonic model is insignificant, and the residuals are homogeneously distributed over the whole region. This implies that the spherical cap harmonic model performs better than the polynomial model especially for a larger region at high latitudes.

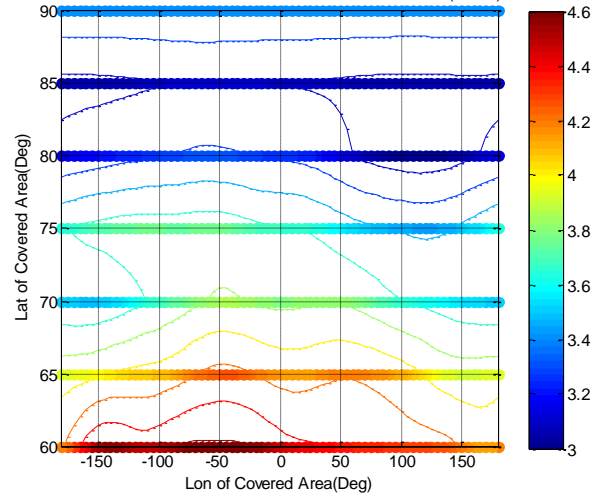


Figure 9: The spatial distribution of the residuals of the spherical cap harmonic model

3.3 The regional ionosphere TEC average

In the spherical cap harmonic model, the coefficient $\tilde{C}_{0,0}$ represents the average of the regional TEC. In order to evaluate the accuracy of the estimated $\tilde{C}_{0,0}$, the regional average TEC value is also estimated using GIM data with (Schaer 1999):

$$\bar{E} = \frac{\sum (\cos \beta * E_{\beta,\gamma})}{\sum \cos \beta} \quad (16)$$

where \bar{E} is the average of the regional TEC estimated with the GIM model, $E_{\beta,\gamma}$ is the TEC of GIM model at the grid point (β, γ) , and $\cos \beta$ is the weight of the grid points at latitude β .

Fig. 10 shows the daily mean of the $\tilde{C}_{0,0}$ coefficients of the spherical cap harmonic model and that of the regional average TEC values estimated with Eq. (16). The line with the star (*) in the upper sub-figure shows the result of the spherical cap harmonic model, while the other line shows that of the GIM model. The correlation coefficient between these two data series is 0.83. The lower sub-figure in Fig. 10 shows the difference between these two data series. The daily mean of the $\tilde{C}_{0,0}$ coefficients of spherical cap harmonic model has a 2.78 TECU bias comparing to that of the GIM model for the same region, while the GIM model has a systematic mapping error of -0.47 TECU as listed in Table 2.

Furthermore, Fig. 10 also discovers that the regional TEC average estimated with two approaches both have the trend of an increasing level as the sunlight moves toward this region during this period. This implies that the solar radiation has significant effect on the production of free electrons.

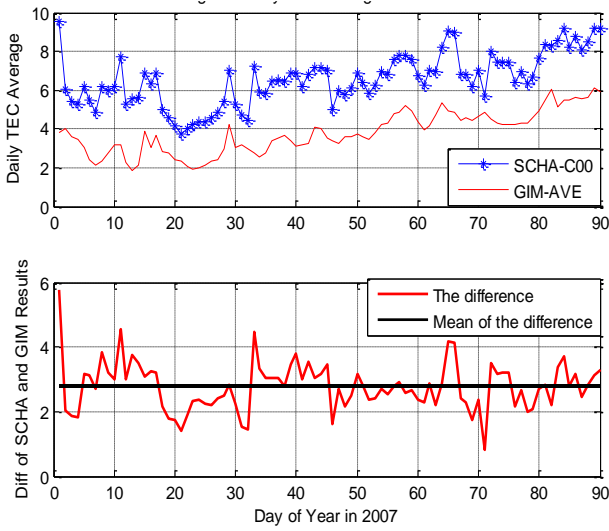


Figure 10: Daily regional TEC average: from the spherical cap harmonic model and GIM interpolated model

One interesting question is whether the zero-degree coefficient of the lower degree spherical function model (LSF) can also indicate the TEC average of the region since this model has a similar expression form with the spherical cap harmonic model? The coefficient series of the lower degree spherical function model is plotted in Fig. 11. As shown, the zero-degree coefficients of the lower degree spherical function model could not indicate the TEC average of the region.

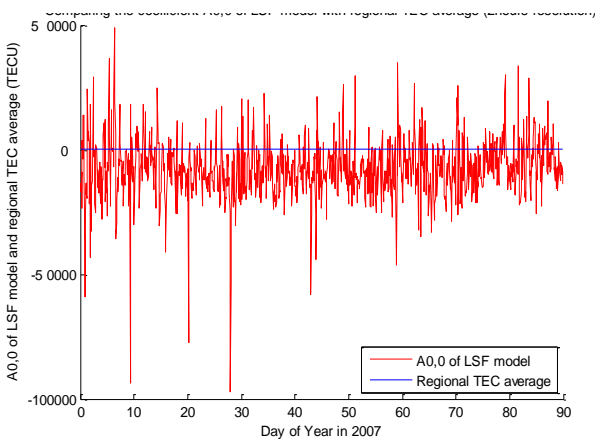


Figure 11: The zero-degree coefficient (A_0^0) of the lower degree spherical function model with 2 hours resolution

3.4 The spectrum analysis of spherical cap harmonic models

In spherical cap harmonic model, the coefficient $\tilde{C}_{0,0}$ represents the average of regional TEC. Fig. 12 shows the mean regional TEC derived from the spherical cap model (the blue line) and the GIM interpolation (the red line) approach with two hours resolution. In order to investigate the periodic property of the spherical cap

harmonic model, based on Fast Fourier Transform (FFT) method, the spectrum analysis is applied to the time series of the estimated coefficients of the spherical cap harmonic model. The results of the spectral analysis of several coefficients are demonstrated as the examples in Fig. 13 and Fig. 14.

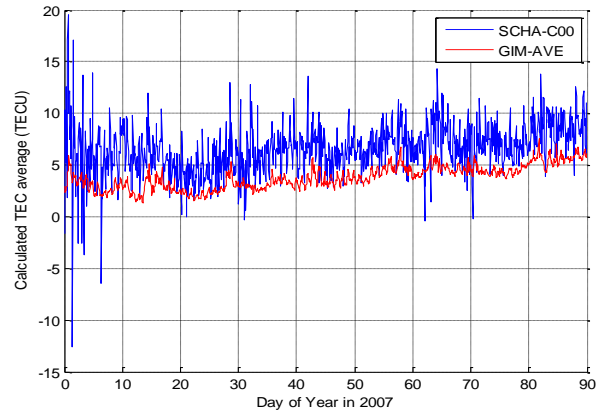


Figure 12: Regional TEC average with 2 hours resolution: from the spherical cap harmonic model and GIM interpolated model

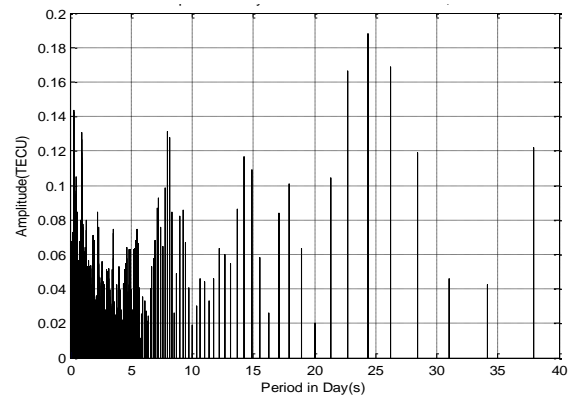


Figure 13: Amplitudes of the regional TEC average from spherical cap harmonic model

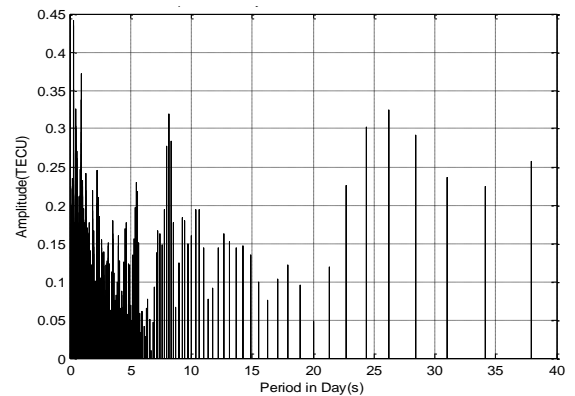


Figure 14a: Amplitudes of the spectral analysis on the coefficients of the spherical cap harmonic model (for the item $\tilde{C}_{1,0}$)

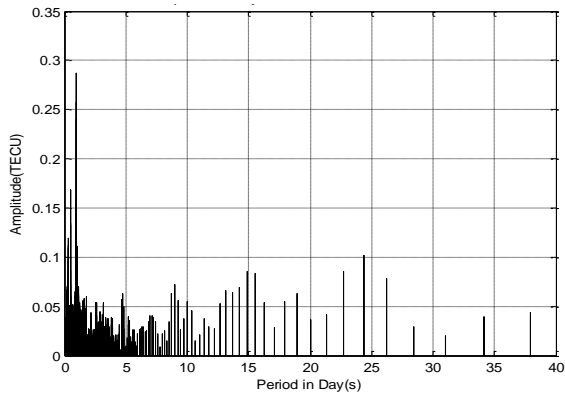


Figure 14b: Amplitudes of the spectral analysis on the coefficients of the spherical cap harmonic model (for the item $\tilde{C}_{1,1}$)

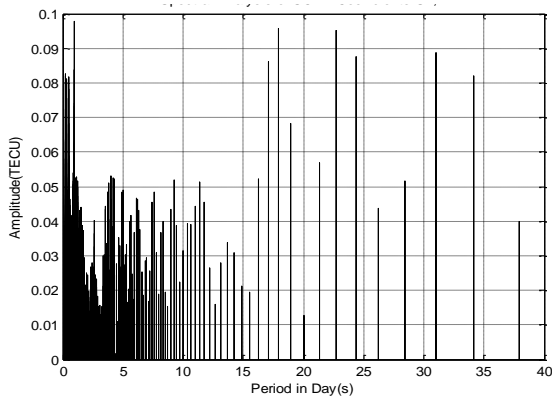


Figure 14c: Amplitudes of the spectral analysis on the coefficients of the spherical cap harmonic model (for the item $\tilde{S}_{1,1}$)

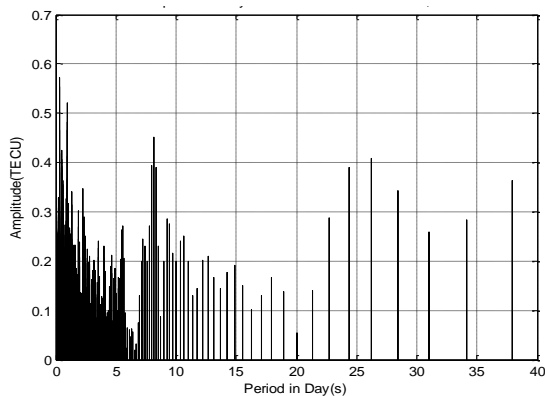


Figure 14d: Amplitudes of the spectral analysis on the coefficients of the spherical cap harmonic model (for the item $\tilde{C}_{2,0}$)

Although this initial study presented in this paper just uses the data of three months, the spectrum components of the coefficients are identifiable. Prominent peaks of the spectrum components may be noticed at a daily period for all coefficients and at around 27-day periods

for some of coefficients. These two spectrum components are related to the well-known ionosphere phenomena (Rishbeth and Garriott 1969). The daily component corresponds to the earth rotation and the period of the hour angle of the Sun. The fact that all coefficients have a noticeable spectrum component of 1-day period indicates that the solar radiation has a strong impact on the ionosphere activity of high latitudes and the arctic region. The ionospheric periods of around 27 days are caused by sunspots co-rotating with the Sun's surface. The associated peak is spread over a certain temporal range because the angular velocity varies with solar latitude.

From Fig. 14, some of coefficients are also seen the spectrum components which, however, could not be related with typical periodicity of global ionospheric activity. For instance, there is a peak around 18 days in Fig. 14c, and a peak of weekly period in Fig. 14d. These spectrum components should be confirmed through using the data covering longer time, and need to be further analysed from physical viewpoint.

It is significant that the periodicities can be identified from the coefficients of the spherical cap harmonic models through the spectrum analysis. The periodicities of the coefficients enable the prediction of the regional TEC values (Liu 2008b).

Similar to these terms presented above, spectrum analysis can be applied to all other coefficients of the spherical cap harmonic models. The spectrum characteristics of various coefficients are different to each other, and need to be analysed one by one.

4. Conclusion and Future Work

This paper presents a first study of applying the spherical cap harmonic model to mapping the ionosphere TEC of high latitudes and the arctic region. Comparing with the conventional regional models, the spherical cap harmonic model has much advantage in mapping the regional TEC of high latitudes as the spherical cap harmonic model is defined in a spherical cap coordinate system. A set of GPS observation data in the high latitudes region and IGS products of the first 90 days in 2007 are exploited to evaluate the spherical cap harmonic model in this study. The effect of the solar activity on the ionosphere of this region is minimal in this period.

The results demonstrate that the spherical cap harmonic model has a comparable mapping accuracy compared to other regional TEC approaches, and has approximately a homogeneous accuracy over the entire region of high latitudes and the arctic area. The property of having no boundary effect is preferred to mapping the TEC over

one large region. In addition, the coefficient $\tilde{C}_{0,0}$ of the spherical cap harmonic model indicates the TEC average of the region, and all of the coefficients have the spectrum characteristics consistent with the well-known ionosphere phenomena. This implies that the coefficients of the spherical cap harmonic model can be predicted based on their spectrum characteristics, therefore the mapping of ionosphere TEC in high latitudes and the arctic region can also be predicted. It is essential to predict the ionosphere TEC for navigation and spatial engineering applications in high latitudes and the arctic region.

However, the interval of three months is a short time-period relating to the variation of the ionosphere. The robustness of the spherical cap harmonic model should be examined during periods with higher ionospheric variability such as auroral activity, enhanced precipitation, ionospheric storms. In future, we will process and analyse the data covering 11 year solar cycle, and investigate further the impact of solar activities and the geomagnetic field on the ionosphere TEC of high latitudes and the arctic region. Moreover, the prediction of the TEC values will be additionally studied in the future using the spectrum characteristics of the ionosphere TEC in high latitudes and the arctic region.

References

- Georgiadiou, Y (1994), *Modeling the ionosphere for an active control network of GPS station*, LGR-series (7), Delft Geodetic Computing Centre, Delft.
- Haines, G.V (1985), *Spherical cap harmonic analysis*, J Geophys Res 90(B3), pp. 2583-2591.
- Haines, G.V (1988), *Computer programs for spherical cap harmonic analysis of potential and general fields*, Comput & Geosci 14 (4), pp. 413-447.
- Komjathy, A (1997), *Global ionospheric total electron content mapping using the global positioning system*, Dissertation, University of New Brunswick.
- Li, J (1993), *The spectral methods in physical geodesy*, Dissertation, Wuhan Technical University of Surveying and Mapping (In Chinese).
- Liu, J (2008), *SCHA analysis and predication of regional ionospheric TEC using ground-based GPS measurements*, Dissertation, Wuhan University (In Chinese).
- Liu, J., Wang Z., Zhang H., Zhu W (2008a), *Comparison and consistency research of regional ionospheric TEC models based on GPS measurements*, Geomat and Inf Sci of Wuhan University 33 (5), pp. 479-483 (In Chinese).
- Liu, J., Wang Z., Wang H., Zhang H (2008b), *Modeling regional ionosphere using GPS measurements over China by spherical cap harmonic analysis methodology*, Geomat and Inf Sci of Wuhan University 33 (8), pp. 792-795 (In Chinese).
- Klobuchar J.A. (1996), *Ionospheric Effects on GPS*, in Parkinson, B.W. and Spilker, J.J. (Eds.), Global positioning system: theory and applications, Volume I. American Institute of Aeronautics and Astronautics, Washington DC.
- Rishbeth, H, Garriott, O. K (1969), *Introduction to ionospheric physics*, Academic Press, New York.
- Sardon E, Rius A, Zarraoa N (1994), *Estimation of the transmitter and receiver differential biases and the ionospheric total electron content from Global Positioning System observations*, Radio Science 29(3): 577-586.
- Schaer, S (1999), *Mapping and predicting the Earth's ionosphere using the global positioning system*, Dissertation, University of Bern.
- Schaer, S., Gurtner W., Feltens J (1998), *IONEX: The IONosphere map Exchange format version 1*, In Proceedings of the IGS AC workshop, Darmstadt, Germany, February 9-11, 1998. Available via the web link: <ftp://igsceb.jpl.nasa.gov/igsceb/data/format/ionex1.pdf>. Accessed at 19 June 2009.
- Wilson BD, Mannucci AJ, Edwards CD (1995), *Subdaily Northern Hemisphere Ionospheric Maps Using an Extensive Network of GPS Receivers*, Radio Science 30: 639-648.

Biography:

Dr. Jingbin Liu is a specialist research scientist in the Department of Navigation and Positioning at the Finnish Geodetic Institute (FGI). In past decade, Dr. Liu has been working on the study of GNSS application and location technologies, and has earned his Bachelor degree (2001), Master degree (2004) and Doctoral degree (2008) in Geomatics Engineering from Wuhan University, China. Currently, his research interests cover various aspects of indoor/outdoor seamless positioning, including GNSS precise positioning, integrated GNSS/inertial sensors positioning, indoor location awareness based on wireless signals, and software defined GNSS receiver technology as well as GNSS-based meteorology. His email is liu.jingbin@fgi.fi.